Electronic Supplementary Material (ESI) for RSC Advances.

Supporting Information

High-Performance Cellulose Nanofibers, Single-Walled Carbon Nanotubes and Ionic Liquid Actuators with a Poly(vinylidene fluoride-*co*-hexafluoropropylene)/Ionic Liquid Gel Electrolyte Layer

Naohiro Terasawa*, Kinji Asaka

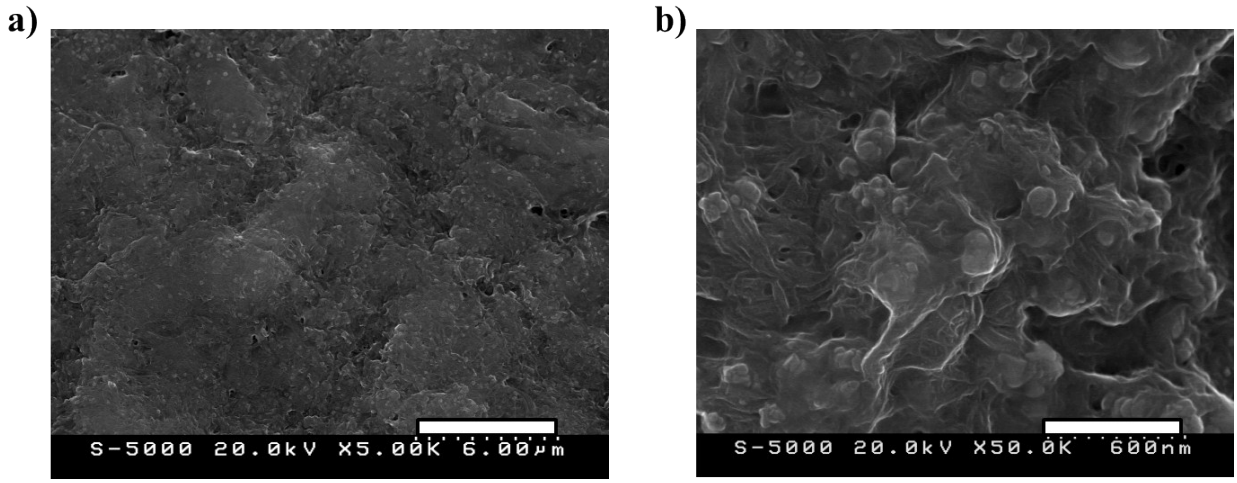

Figure S1. Scanning electron microscopy micrographs (20.0 kV) of PVdF(HFP)/SWCNT/EMI[BF_4] = 80/50/120 electrode layers with (a) magnification = 5,000x and (b) magnification = 50,000x.

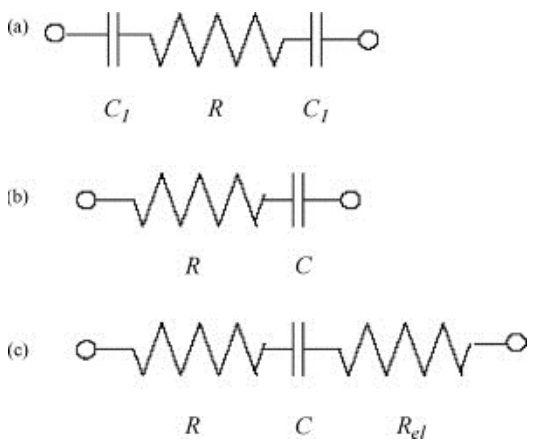

Figure S2. Three equivalent circuit models for the CNF/SWCNT/IL actuator, where C_1 and C denote the specific capacitance ($C = C_1/2$), R denotes the ionic resistance and R_{el} denotes the electrode resistance.

Figure S2 presents the equivalent circuit models for the CNF/SWCNT/IL actuators. The model in **Figure S2(a)** comprises the specific capacitance C_1 between the CNF/SWCNT/IL electrode layer and the resistance R associated with the PVdF(HFP) or CNF/IL electrolyte layer. **Figure S2(b)** depicts a more simplified model in which the two capacitances C_1 are replaced by a single capacitance C (= $C_1/2$). When a triangular voltage with an amplitude of $\pm A$ and frequency f is applied to the equivalent circuit depicted in **Figure S2(b)**, the maximum accumulated charge $Q(f)$ can be expressed as follows [S1]:

$$Q(f)/Q_0 = 1 - 4CRf\,(1 - \exp(-1/4CRf)), \qquad \text{(S1)}$$

where Q_0 is the accumulated charge at the low-frequency limit. If the strain ε in the electrode layer is proportional to the accumulated charge, it can be calculated as follows:

$$\varepsilon = \varepsilon_0\, Q(f) / Q_0, \qquad \text{(S2)}$$

where ε_0 denotes the strain at the low-frequency limit.

While considering conduction in the electrode layer, it is necessary to account for the electrode resistance in the equivalent circuit. If the electrode resistance is explicitly treated, the equivalent circuit should be treated as a distributed transmission line [S2]. Herein, we assumed that the electrode resistance comprises a resistance element R_{el}, as depicted in **Figure S2(c)**. Thus, R in **Eq. (S1)** can be replaced by $R + R_{el}$.

To evaluate the double-layer charging kinetic model, the double-layer capacitance of the CNF/SWCNT/IL electrode and the ionic resistance of the PVdF(HFP)/IL gel electrolyte layers were measured. Further, the frequency dependence of the strain was calculated using **Eqs. (S1)** and **(S2)**.

Figure 7(a) depicts the frequency dependence of the measured strain values using the simulation results for the BB/SWCNT/EMI[BF_4] electrodes and the PVdF(HFP)/EMI[BF_4] electrolyte actuators. Curve A was calculated using the model denoted in **Figure S2(b)**, and **Table S1** summarises the simulation parameters, whereas Curve B was calculated using the model depicted in **Figure S2(c)**; further, the simulation parameters are presented in **Table S2**. **Figure 7(a)** clearly denotes that the frequency dependence of the strain was well reproduced by Curve B. Similar results were obtained for the LB/SWCNT/EMI[BF_4] and the PVdF(HFP)/EMI[BF_4] electrolyte actuators or the CNF/SWCNT/EMI[CF_3SO_3] electrodes and the PVdF(HFP)/EMI[CF_3SO_3] electrolyte actuators. To fit the strain values in the low-frequency limit in **Figure 7(a)**, appropriate values were selected for ε_0 in **Eq. (S2)**; these values are presented in **Table S2**.

To optimise the performance of the actuator, the results summarised in **Tables S1** and **S2** should be considered from both the kinetic and static perspectives. From the kinetic perspective, the frequency dependence of the strain can be determined via electrochemical charging, as denoted in **Figure 7(a)**. Obtaining good fits generally requires consideration of the electrode and electrolyte resistances. Further, the response of the CNF/SWCNT/IL electrodes and the PVdF(HFP)/IL electrolyte actuators can be improved by fabricating electrodes and electrolytes with high conductivity values.

To evaluate the double-layer charging kinetic model, the double-layer capacitance of the CNF/SWCNT/IL electrode and the ionic resistance of the CNF/IL gel electrolyte layers were measured. The frequency dependence of the strain was calculated using **Eqs. (S1)** and **(S2)**.

Figure 7(b) denotes the frequency dependence of the measured strain values along with the simulation results for the BB/SWCNT/EMI[CF_3SO_3] electrodes and BB/EMI[CF_3SO_3] electrolyte actuators. Curve A was calculated using the model presented in **Figure S2(b)**, and **Table S3**

summarises the simulation parameters. Curve B was calculated using the model denoted in **Figure S2(c)**, and the simulation parameters are presented in **Table S4**. It is clear from **Figure 7(b)** that the frequency dependence of the strain is well reproduced by Curve A (>1 Hz). Similar results were obtained for the LB/SWCNT/EMI[CF_3SO_3] electrodes and the LB/EMI[CF_3SO_3] electrolyte actuators or for the CNF/SWCNT/EMI[BF_4] electrodes and the CNF/EMI[BF_4] electrolyte actuators. To fit the strain values in the low-frequency limit in **Figure 7(b)**, appropriate values were selected for ε_0 in **Eq. (S1); Table S3** presents these values.

To optimise the performance of the actuator, the results summarised in **Tables S3** and **S4** should be considered from both the kinetic and static components. From the kinetic perspective, the frequency dependence of the strain can be determined through electrochemical charging, as denoted in **Figure 7(b)**. Obtaining good fits generally requires consideration of the electrolyte resistance. The response of the CNF/SWCNT/IL electrodes or the CNF/IL electrolyte actuators can be improved by fabricating electrolytes with high conductivities.

Table S1. Simulation parameters of the CNF/SWCNT/IL electrodes and the PVdF(HFP)/IL electrolyte model neglecting the electrode resistance.

CNF/IL	C_{SWCNT} (F g^{-1})	C (F cm^{-2})	κ (mS cm^{-1}) [a]	R (Ω cm^2)	ε_0 (%)	CR (s)
LB/[BF_4]	35.1	0.1131	2.8	0.714	0.44	0.3969
BB/[BF_4]	35.1	0.091	2.8	0.714	0.76	0.065
LB/[CF_3SO_3]	33.2	0.1882	4.4	0.455	0.18	0.086
BB/[CF_3SO_3]	31.5	0.2050	4.4	0.455	0.14	0.093

[a] ref. [S3]

Table S2. Simulation parameters of the CNF/SWCNT/IL electrodes and the PVdF(HFP)/IL electrolyte model considering the electrode resistance.

IL	C (F cm^{-2})	R_{el}(Ω cm^2)	$R+R_{el}$ (Ω cm^2)	$C(R+R_{el})$ (s)
LB/[BF_4]	0.1131	3.4	4.11	0.465
BB/[BF_4]	0.091	6.8	7.51	0.683
LB/[CF_3SO_3]	0.1882	4.4	4.86	0.915
BB/[CF_3SO_3]	0.2050	9.3	9.76	2.001

R_{el} = area of the electrode film (cm^2)/ [electrical conductivity (S cm^{-1}) × thickness of the electrode film (cm)] [S1].

Table S3 Simulation parameters of the CNF/SWCNT/IL electrodes and the CNF/IL electrolyte model ignoring the electrode resistance.

CNF/IL	C_{SWCNT} (F g^{-1})	C (F cm^{-2})	κ (mS cm^{-1})	R (Ω cm^2)	ε_0 (%)	CR (s)
LB/[BF_4]	35.1	0.1131	3.9	1.41	0.44	0.1595
BB/[BF_4]	35.1	0.091	4.6	1.19	0.76	0.1083
LB/[CF_3SO_3]	33.2	0.1882	3.3	1.67	0.18	0.3143
BB/[CF_3SO_3]	31.5	0.2050	3.9	1.41	0.14	0.2337

Table S4 Simulation parameters for the CNF/SWCNT/IL electrodes and the CNF/IL electrolyte model that considers electrode resistance.

IL	C (F cm^{-2})	R_{el}(Ω cm^2)	$R+R_{el}$ (Ω cm^2)	$C(R+R_{el})$ (s)
LB/[BF_4]	0.1131	3.4	4.81	0.544
BB/[BF_4]	0.091	6.8	7.99	0.727
LB/[CF_3SO_3]	0.1882	4.4	6.07	1.142
BB/[CF_3SO_3]	0.2050	9.3	10.71	2.196

R_{el} = area of the electrode film (cm^2) /[electrical conductivity (S cm^{-1}) × thickness of the electrode film (cm)] [S1].

References

[S1] I. Takeuchi, K. Asaka, K. Kiyohara, T. Sugino, K. Mukai, T. Fukushima and T. Aida, *Electrochim Acta,* 2009, **53**, 1762–1768.

[S2] K. Takagi, Y. Nakabo, Z.-W. Luo, and K. Asaka, *Proceedings of the SPIE, Electroactive Polymer Actuators and Devices (EAPAD)*, 2007, **6524**, 652416-1-652416-8.

[S3] N. Terasawa, I. Takeuchi, and H. Matsumoto, Electrochemical properties and actuation mechanisms of actuators using carbon nanotube-ionic liquid gel. *Sens Actuators B*, 2009, **139,** 624–630.